Analytical Model for Shear Critical Reinforced Concrete Members under Static Loads

W. Chung and S.H. Ahmad[1]

In this investigation a nonlinear finite element model is developed for predicting the complete load-deflection response of shear critical reinforced concrete members. The nonlinear finite element model employs a biaxial stress-strain constitutive relationship of concrete based on equivalent uniaxial approach developed in this study and a simplified bilinear stress-strain relationship of reinforcing steel. The main feature of the model is its ability to predict the post-peak load-deflection response of shear critical reinforced concrete members failing under a diagonal tension. The computational procedure developed employs the secant stiffness method and a non-iterative algorithm. The predictions of the model are compared with the available experimental data and the comparisons are judged to be in good agreement.

INTRODUCTION

Shear (diagonal tension) failure of reinforced concrete structures has been generally accepted as a sudden and brittle failure because of the lack of ductility, which can be broadly defined as the ability to undergo large deformations without loss of significant strength. However, the appropriate placement of web reinforcement can effectively prevent the sudden and brittle failure under shear loads. With the development of concrete with higher strengths, issues regarding the shear behavior and associated failures are becoming increasingly important. Recent analytical research efforts for studying the behavior of reinforced concrete structural members has concentrated on development of theories to predict the failure mechanisms under shear loads. The notable theories proposed for modeling the behavior of reinforced concrete structural members include the Modified Compression Field Theory (MCFT) as proposed by Vecchio and Collins [1], the Softened Truss Model as proposed by Hsu [2], the Compressive Force Path Theory as proposed by Kotsovos [3,4] and the Strut and Tie model by COPPE and CEB [5].

Although there is substantial research activity to address some of the concerns regarding shear (diagonal tension) behavior of reinforced concrete members, there is no generally accepted theory for predicting with sufficient reliability the behavior and the associated failure. Moreover, the analytical models do not exhibit the ability to predict the post-peak displacement softening behavior under diagonal tension failure.

In this investigation, a nonlinear finite element model is developed for predicting the complete load-deflection response of reinforced

1. Dept. of Civil Engineering, North Carolina State University, NC, USA 27612.

Scientia Iranica, Vol. 1, No. 2, © Sharif University of Technology, July 1994.

concrete members. The deflection incremental approach, based on the secant stiffness method, is developed to predict the post-peak displacement softening behavior for shear critical reinforced concrete members. The nonlinear finite element model employs a biaxial stress-strain constitutive relationship of concrete, based on an equivalent uniaxial approach developed in this study, and a simplified bilinear stress-strain relationship of reinforcing steel. The main feature of the model is its ability to predict the post-peak load-deflection response of reinforced concrete members failing under diagonal tension. This post-peak behavior is a relative measure of shear ductility. The model is applicable only to short term loading and utilizes a plane stress element with sheared stiffness approach for modeling the reinforced concrete member. The predictions of the model are compared with the available experimental data.

ANALYTICAL MODEL

Constitutive Model for Concrete

A biaxial stress-strain law for concrete is used which is based on an equivalent uniaxial approach (i.e.,the Poisson's effect is ignored). Effects of repeated loading and creep are not included. A simplified strength and strain criterion for biaxial stresses is developed and then use is made of the fractional equation form proposed by Ahmad and Shah [6], for uniaxial stress-strain relationship of concrete in compression, to obtain the complete stress-strain relationship under biaxial stresses.

The strength criterion under biaxial stresses for the compression-tension region of the biaxial stress space [7] is given by

$$\sigma_{1p} = 1 + 0.824\left(\frac{\sigma_{2p}}{\sigma_0}\right) - 109.4\left(\frac{\sigma_{2p}}{\sigma_0}\right)^2, \tag{1}$$

where σ_{1p}, σ_{2p} are the stresses at peak and σ_0 is an uniaxial compressive strength of concrete. The strength criterion for compression-compression region is given by

$$\sigma_{1p} = 1 + 0.458\left(\frac{\sigma_{2p}}{\sigma_0}\right) + 0.164\left(\frac{\sigma_{2p}}{\sigma_0}\right)^2 - 0.395\left(\frac{\sigma_{2p}}{\sigma_0}\right)^3. \tag{2}$$

Comparison of the biaxial strength envelope predicted by Equations 1 and 2 with the experimental data [8,9] is shown in Figure 1.

The equations for the concrete strain criterion under biaxial stresses were obtained by using the experimental data of Kupfer et al. [10]. The equation for predicting the strains (ε_{1p}) at maximum stress are given by

$$\varepsilon_{1p} = \varepsilon_0 - 0.00447\left(\frac{\sigma_{2p}}{\sigma_{1p}}\right) - 0.0841\left(\frac{\sigma_{2p}}{\sigma_{1p}}\right)^2 \quad c.c. \sim 0.99, \tag{3}$$

for compression-tension, where *c.c.* is a correlation coefficient, the ratio σ_{2p}/σ_{1p} is considered to be negative and $\varepsilon = 0.001648 + 0.000114\sigma_0$ (σ_0 is in ksi units), and

$$\varepsilon_{1p} = \varepsilon_0 - 0.00278\left(\frac{\sigma_{2p}}{\sigma_{1p}}\right) - 0.00235\left(\frac{\sigma_{2p}}{\sigma_{1p}}\right)^2 \quad c.c. \sim 0.99, \tag{4}$$

for compression-compression, where *c.c.* is a correlation coefficient and the ratio σ_{2p}/σ_{1p} is considered to be positive.

Once the stresses and strains at the maximum peak stress under biaxial stresses state are computed, the fractional equation [6] is used to express the stress-strain relationship under biaxial stresses. The compressive stress-strain relation is given by

$$f_c = \sigma_{1p}\frac{Ax + (B-1)x^2}{1 + (A-2)x + Bx^2}, \tag{5}$$

where

$x = \varepsilon/\varepsilon_{1p}$,

f_c = compressive stress in concrete,

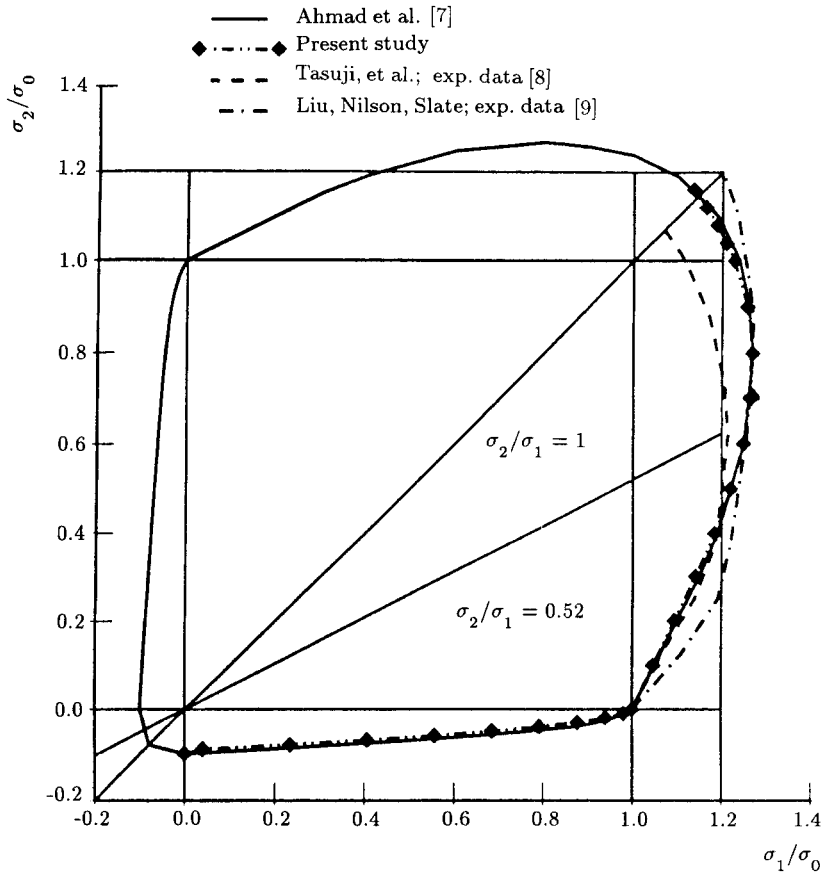

Figure 1. Comparison of analytical and experimental biaxial strength envelope.

σ_{1p} = peak strength of concrete under biaxial stresses,
A, B = calibrating parameters,
ε = concrete strain
ε_{1p} = strain at the maximum stress under biaxial stresses.

The constants for ascending and descending portions of the compressive stress-strain curves under biaxial stresses were calibrated from the limited experimental data [7,10]. The constants for the biaxial stress-strain relationship are as follows for compression-tension and $\varepsilon \leq \varepsilon_{1p}$,

$$A_{1t} = 2.2 - 0.211\sigma_0 + 0.017\sigma_0^2 - 0.0045\sigma_0^3,$$
$$A_{1t} > 1.321,$$
$$B_{1t} = 1.869 - 0.443\sigma_o + 0.039\sigma_0^2 - 0.00119\sigma_0^3,$$
$$B_{1t} > 0.187, \qquad (6)$$

for compression-tension and $\varepsilon \geq \varepsilon_{1p}$,

$$A_{2t} = e^{(2.74 - 0.683\sigma_0 + 0.0227\sigma_0^2)},$$
$$0.094 \leq A_{2t} \leq 2.0,$$
$$B_{2t} = B_{20}\left[1 - 4.617\left(\frac{\sigma_{2p}}{\sigma_0}\right) - 54.17\left(\frac{\sigma_{2p}}{\sigma_0}\right)^2\right], \qquad (7)$$

where

$$B_{20} = 0.6 + 0.07\sigma_0,$$
$$\sigma_0 \leq 5 \text{ ksi (34.5 MPa)},$$
$$B_{20} = 0.729 + 0.0726\sigma_0^2 - 0.0067\sigma_0^2 + 2.1^*10^{-4}\sigma_0^3,$$
$$\sigma_0 > 5 \text{ ksi},$$
$$B_{2t} \leq 1.0,$$
σ_0 = uniaxial strength of concrete (ksi)
σ_{2p} = tensile stress at peak.

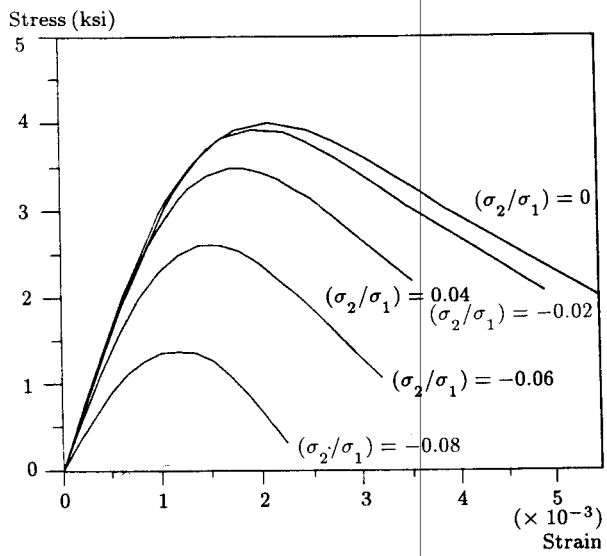

Figure 2. Stress-strain curves for different stress ratios under compression-tension stresses as predicted by Equation 5 (1 ksi = 6.895 MPa).

For compression-compression and $\varepsilon \leq \varepsilon_{1p}$,

$$A_{1c} = A_{1t},$$
$$B_{1c} = B_{1t}. \tag{8}$$

and for compression-compression and $\varepsilon \geq \varepsilon_{1p}$,

$$A_{2c} = A_{2t},$$
$$B_{2c} = 1.25B_{20}. \tag{9}$$

Figures 2 and 3 represent compressive stress-strain curves under biaxial stresses as predicted by the biaxial stress-strain law based on the equivalent uniaxial approach. These figures show the effect of transverse compressive strain and transverse tensile strains on the strength and the stress-strain behavior of plain concrete. Ascending and descending portions and the maximum compressive stress of stress-strain curve under compression-tension stresses (Figure 2) are sensitive to the biaxial stress ratio σ_2/σ_1. The ascending portion of stress-strain curves under compression-compression stresses is not sensitive to the biaxial stress ratio σ_2/σ_1, however the maximum compressive stress and the descending portions are sensitive to the biaxial stress ratio (Figure 3). Plain concrete in tension is modeled by the uniaxial stress-strain relationship as follows:

$$\frac{f_t}{f'_t} = e^{(1-\varepsilon_t/\varepsilon'_t)}, \tag{10}$$

where f_t = tensile stress, f'_t = maximum tensile stress, ε_t = tensile strain, and ε'_t = tensile strain at the maximum tensile stress (peak tensile strain).

It is assumed that a modulus of elasticity E_t under a tension stress is the same as that under a compression stress E_c before cracking. For a given f'_t value, the ε'_t value is computed by dividing f'_t by E_c. The value of E_c for a given concrete strength σ_0 is computed by $E_c = 27.5\ w^{1.5}\sqrt{\sigma_0}$ as recommended by Ahmad and Shah [6]. The comparison of Equation 10 and the experimental result of Gopalaratnam and Shah [11] is shown in Figure 4.

For biaxial stresses, the presence of compressive stresses has an effect on the tensile stress-strain relationship of concrete. Due to the lack of experimental verification of this effect, it has been ignored and, hence, the uniaxial tensile stress-strain relationship, Equation 10, has been used for biaxial stress states.

The effect of reinforcement amount on the tensile stress-strain of concrete was modelled as per the suggestion of Stevens et al. [12] and the

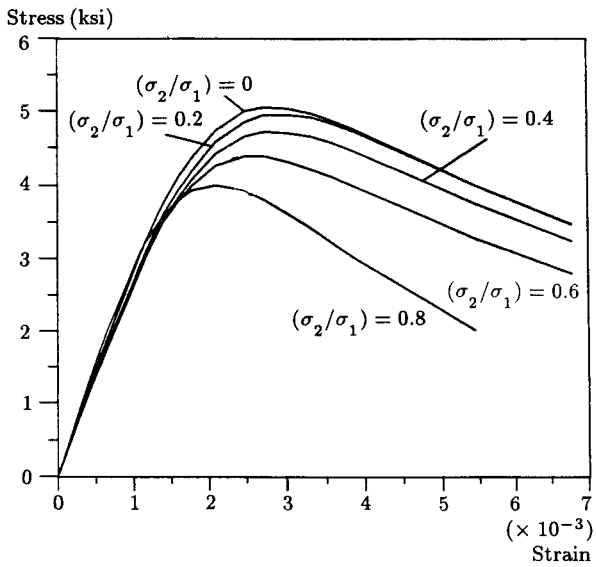

Figure 3. Stress-strain curves for different stress ratios under compression-compression stresses as predicted by Equation 5 (1 ksi = 6.895 MPa).

following equation has been suggested:

$$\frac{f_t}{f_t'} = (1-\alpha)e^{-\lambda_t(\varepsilon_t - \varepsilon_t')} + \alpha, \qquad (11)$$

where f_t' = maximum tensile stress, $\alpha = 75\frac{\rho_s}{d_b}$ (in mm), ρ_s = steel ratio , $\rho_s = \frac{A_s}{A_c}$, d_b = diameter of bar (in mm), A_c = distributed across area (in mm^2), A_s = steel area (in mm^2), ε_t = tensile strain in concrete and ε_t' = maximum tensile strain in concrete.

The rate of decay parameter λ_t is

$$\lambda_t = \frac{270}{\sqrt{\alpha}}, \quad \lambda_t \leq 1000.$$

Note that Equation 11 is not applicable for plain concrete.

Figure 5 shows the effect of reinforcement amount on the tensile stress-strain curve of concrete as predicted by Equation 11. Also shown in this figure is the prediction as per MCFT model [1] which is independent of the amount of reinforcement and is applicable when a large amount of well distributed reinforcement is present.

Constitutive Model for Reinforcing Steel

The stress-strain curve of reinforcing steel is modeled by a bilinear curve in tension and compression (Figure 6). Steel stress is computed as

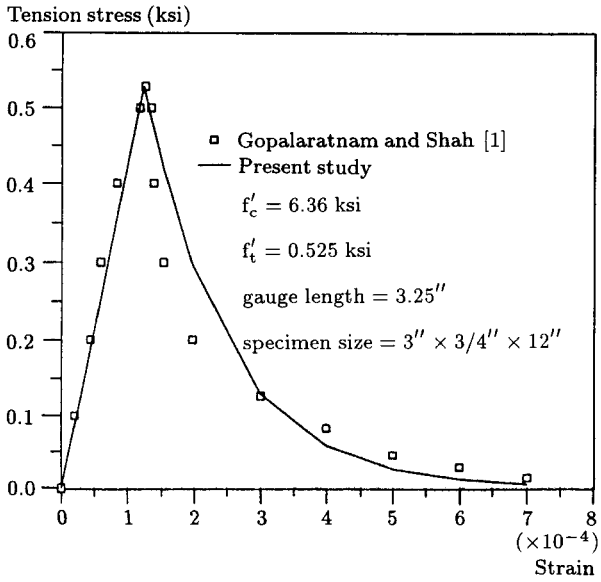

Figure 4. Comparison of Equation 10 and the experimental result of [11](1 ksi = 6.895 MPa).

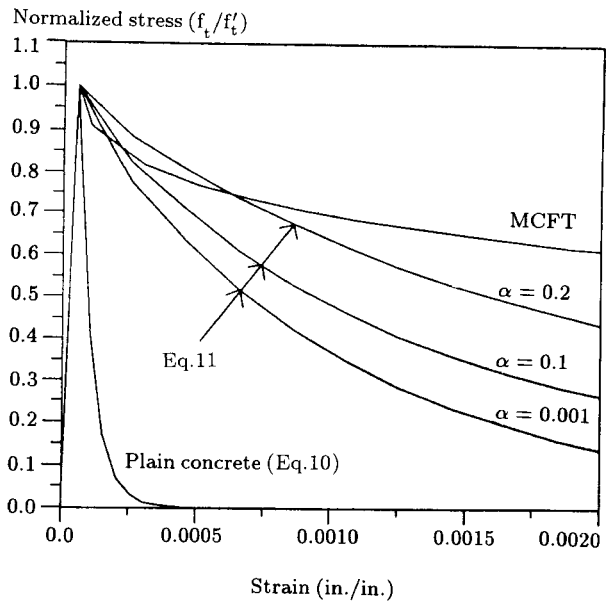

Figure 5. Effect of reinforcement amount tensile stress-strain curve of concrete.

follows:

$$f_s = E_s\varepsilon_s, \qquad \text{for} \quad \varepsilon_s \leq \varepsilon_{sy}, \qquad (12)$$

where

E_s = modulus of steel,
ε_s = strain in steel,
ε_{sy} = yield strain in steel,

$$f_s = f_y = E_s'\varepsilon_s, \qquad \text{for} \quad \varepsilon_s > \varepsilon_{sy},$$
$$f_y = \text{yield of steel}, \qquad (13)$$

where E_s' = secant modulus of steel.

Finite Element Approach

Various development approaches of Nonlinear Finite Element Method for reinforced concrete structures have been utilized, differing in such aspects as constitutive modeling of concrete and reinforcing steel, stiffness formulation (tangent stiffness versus secant stiffness) and different element preference. To avoid difficulties associated with predicting the complete behavior of reinforced concrete members, finite element approaches have ignored the modelling

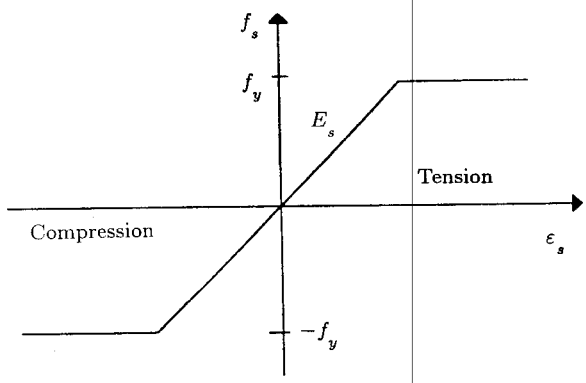

Figure 6. Constitutive model for reinforcing steel.

of softening portions of the compressive and tensile stress-strain relationships of concrete. However, some recent works [13,14] have accounted for the softening portion through relatively complicated algorithms, for example, Pramono [14] uses the Pseudo-Force algorithm.

There are basically two methods employed in the finite element analyses, the load increment method and the displacement increment method. Both methods can utilize the secant stiffness formulation which allows easier adaptation to a nonlinear analysis capability with stable solutions. It should be noted that, although the tangent stiffness formulation gives fast convergency for every incremental step, it has computational difficulties in the displacement softening portion of the load-displacement response. Although the model employing the load increment method gives good results [15], it is not capable of predicting the post-peak deformation softening region of the load-deflection response of reinforced concrete structural members.

In the development of the finite element method model, a displacement increment method using a secant stiffness approach is used. The smeared cracking model [13] for a crack representation was used, in which a strength criterion is used for crack initiation. In the development of the model in this study, the crack rotation concept is applied and Poisson's effect of the cracked element has been ignored. Therefore, a reinforced concrete element can be modeled as a combination of the stiffness of concrete element and steel element. The inclusion of stirrup with reinforcement ratio, ρi is done by superimposing the steel stiffness to the concrete element stiffness or reinforced concrete stiffness, as the case may be. In the model, perfect bond between steel and concrete is assumed and dowel action is ignored. Since the nonlinear finite element program developed is based on the secant stiffness approach, it utilizes linear elastic algorithms. Development of linear elastic procedures is well documented in literature [16,17]

For predicting the post-peak deformation portion of the load-deflection response of reinforced concrete structural members, the computational procedure based on the displacement increment approach is developed [18]. The algorithm of the displacement increment procedure of the nonlinear finite element method using the secant stiffness approach is shown in Figure 7.

In the conventional procedure, a residual stress $d\sigma$ for every iteration is used so that convergence is reached when the residual stress approaches zero. Therefore, the computational procedure using the residual stress approach needs several iterations for every incremental step. Since the computational procedure developed employs the secant stiffness method and

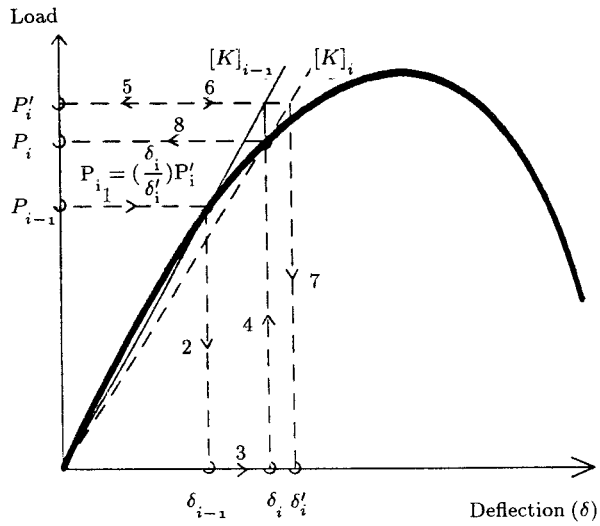

Figure 7. Algorithm of displacement increment procedure for finite element method using the secant stiffness approach.

a non-iterative algorithm, it reduces computing time and also simplifies the computations.

Before starting the first displacement step δ_1, a unit total load is applied to the structure and an initial global structural matrix $[K]_{ini}$, a displacement vector $\{d\}_{ini}$, and a load vector $\{p\}_{ini}$, are calculated by conventional linear procedure. The matrix and vectors are used for the first displacement step δ_1. After that, previous known values are used to a current displacement step, In the i-th displacement step δ_i, the previous global stiffness matrix $[K]_{i-1}$, the previous load vector $\{P\}_{i-1}$, and the previous displacement vector $\{d\}_{i-1}$, are known values. Because the secant stiffness approach is being used, the step factor $(SF)_i$ with respect to the i-th displacement step can be obtained by

$$(SF)_i = \frac{\delta_i}{\delta_{i-1}}, \tag{14}$$

where δ_{i-1} = a previous displacement step at the assigned node and δ_i = a current displacement step at the assigned node.

As the structural stiffness is a linear, total external load in current iteration, P_i', it can be written as

$$P_i' = P_{i-1}(SF)_i, \tag{15}$$

where P_{i-1} is a previous total external load.

Thus, new deflection vector, $\{d\}_i$, and load vector, $\{p'\}_i$, can be calculated by simply multiplying the step factor $(SF)_i$ with the previous deflection and load vectors, i.e., use of the proportionality rule. The new deflection vector $\{d\}_i$ and load vector $\{p'\}_i$ are given by

$$\{d\}_i = \{d\}_{i-1}(SF)_i, \tag{16}$$

$$\{p'\}_i = \{p\}_{i-1}(SF)_i, \tag{17}$$

where $\{d\}_i$ = the deflection vector in i-th step and $\{p'\}_i$ = the load vector in first iteration of i-th step.

The concrete and steel material stiffness matrices, $[D]_c$ and $[D]_s$, based on the constitutive models of this study, are evaluated with respect to the principal axes using a new displacement vector, $\{d\}_i$. The detailed procedure for obtaining the material stiffness matrix, element stiffness matrix and the global structure stiffness matrix $[K]_i$, has been described in the literature [15,16,17]. The new nodal point displacement vector $\{d'\}_i$ is found by use of the governing equation

$$\{d'\}_i = [K]_i^{-1}\{p'\}_i. \tag{18}$$

While in the conventional procedure, the total load for the i-th displacement step is obtained by the sum of the internal load of each element, here it is determined by multiplying the P' with the ratio of the displacement at i-th step to the current displacement. The total load for the i-th displacement step is given by

$$P_i = P_i' \frac{\delta_i}{\delta_i'}, \tag{19}$$

where δ_i' = current displacement at assigned node and δ_i = i-th displacement step at assigned node.

The flow chart of the algorithm of displacement increment procedure of the finite element method is shown in Figure 8. The displacement increment procedure using the secant stiffness approach exhibits fast convergency and is stable even if the deflections are at and beyond the peak load. It converges in only one iteration for every additional deflection step in the pre- and post-peak regions of the load deflection curve as opposed to the load increment procedure, where the number of iterations to converge increase as the load step is increased. The computing time of the deflection increment method is hundreds of times faster than that of the load increment method for ten comparable increment steps [18].

RESULTS

A deep beam $100 \times 1600 \times 1600$ mm ($4 \times 63 \times 63$ in) was tested by Leonhardt and Walther [19]. The beam was simply supported and was subjected to a uniformly distributed load along the top (Figure 9). The vertical reinforcement was

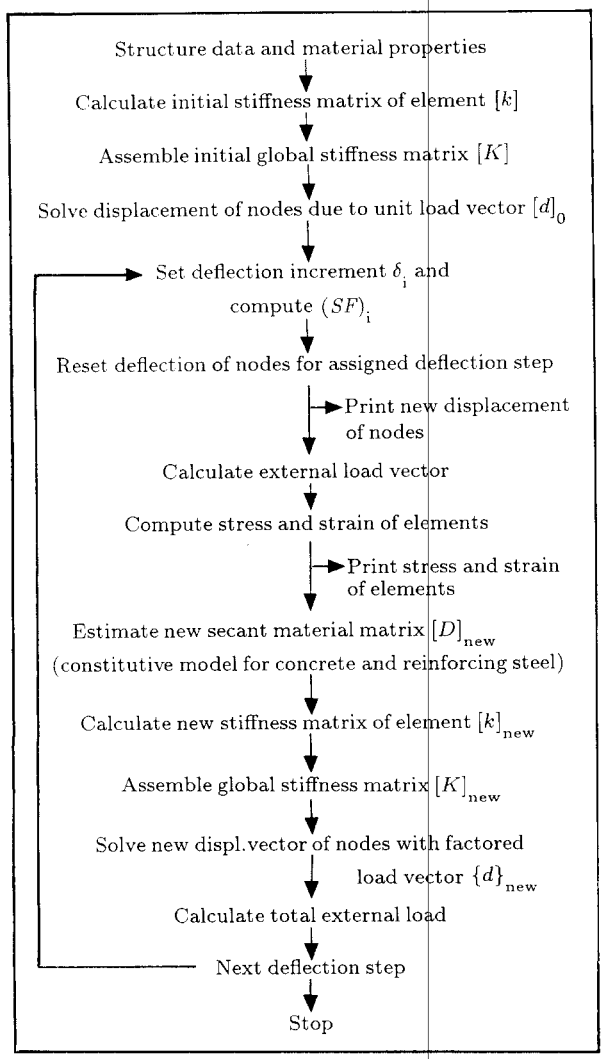

Figure 8. Flowchart of displacement increment procedure for finite element method.

uniform throughout the span ($\rho_y = 0.00175$). The horizontal reinforcement was heavier in the lower regions ($\rho_x = 0.01787$) and lighter in the upper regions ($\rho_x = 0.00175$). The compressive strength of concrete (f'_c) was 4.3 ksi (29.6 MPa). This specimen represented a membrane structure with the smeared reinforcement whose behavior would be dependent on the nonuniform nature of the stress and strain fields generated within the beam. Due to symmetry, only half of the beam was modeled by using 128 four node rectangular plane stress elements for concrete and reinforced concrete elements. The reinforced concrete elements were modeled by using the smeared reinforcement approach, i.e. the reinforcement was smeared in the elements. The tensile strength of concrete (f'_t) was estimated to be $4\sqrt{\sigma_0}$ as recommended by Vecchio [15].

The comparisons of the analytically predicted results with those obtained experimentally is shown in Figure 9. Furthermore, it can be seen that analytical results obtained by using the concrete constitutive model developed in this study and the MCFT are in good agreement with the experimental results. The figure shows that the displacement increment finite element model based on the secant approach exhibits the capability of predicting the post-

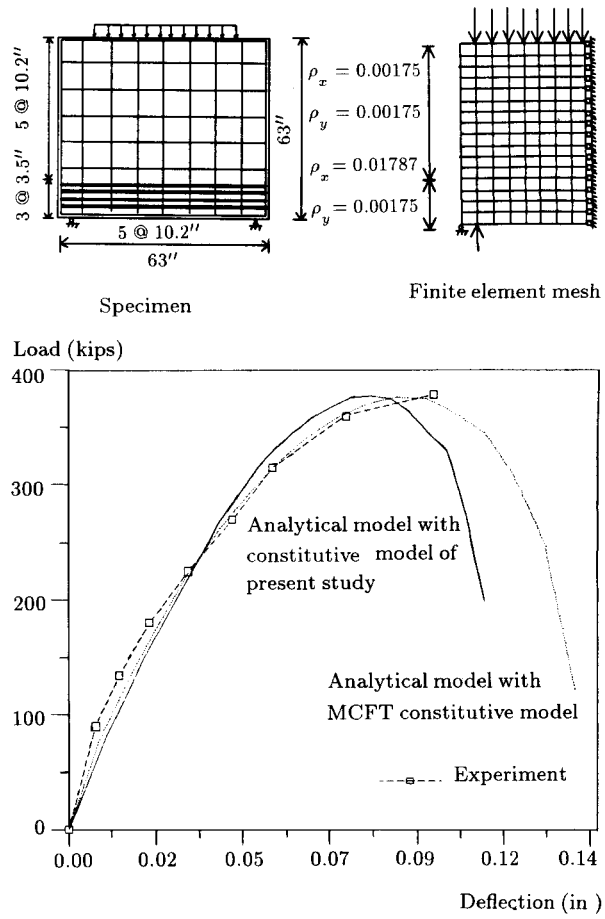

Figure 9. Comparison of load-midspan deflection response for Leonhardt and Walther [19] deep beam specimen with the predictions of the analytical model developed in this study.

peak deformation softening portion of the load-deflection response.

It should be pointed out that the constitutive model of Vecchio and Collins [1] in MCFT, when used with the displacement increment finite element method model developed in this study, shows reasonably good predictive capability for this particular case, because the test specimen is very heavily reinforced ($\alpha = 0.026$).

A series of beams were tested by Bresler and Scordelis [20]. One of the beams, BS1, described in Figure 10, was heavily reinforced with stirrups. The beam was designed to experience a concrete shear failure when simply supported and subjected to a concentrated load at the midspan.

The beam was modeled using 120 rectangular elements and 40 bar elements. The longitudinal reinforcement was modeled in a discrete manner using the bar elements, while the shear reinforcement was included in the properties of the rectangular elements and thus modeled as a smeared element. The web reinforcement ratio ($\rho_y = 0.1$) was used in the smeared element to reflect the effect of reinforcement. The values of the concrete tensile strength (f'_t) and the shear retention factor (μ) used in the model were $4\sqrt{\sigma_0}$ and 0.05, respectively. The shear retention factor is a multiplier to the shear modulus (G_c) in the material matrix and the product of the shear retention factor and the shear modulus represents the shear stiffness of cracked concrete. Since the shear span-depth ratio a/d is 4.2, a flexural behavior was predominant for the load-deflection response and overall behavior of the beam.

The predicted and observed load deflection response curves for the beam are shown in Figure 11. From this figure it can be seen that the analytical model developed in this study seems to accurately predict the experimentally observed response of the beam with web reinforcement. Note that predictions by

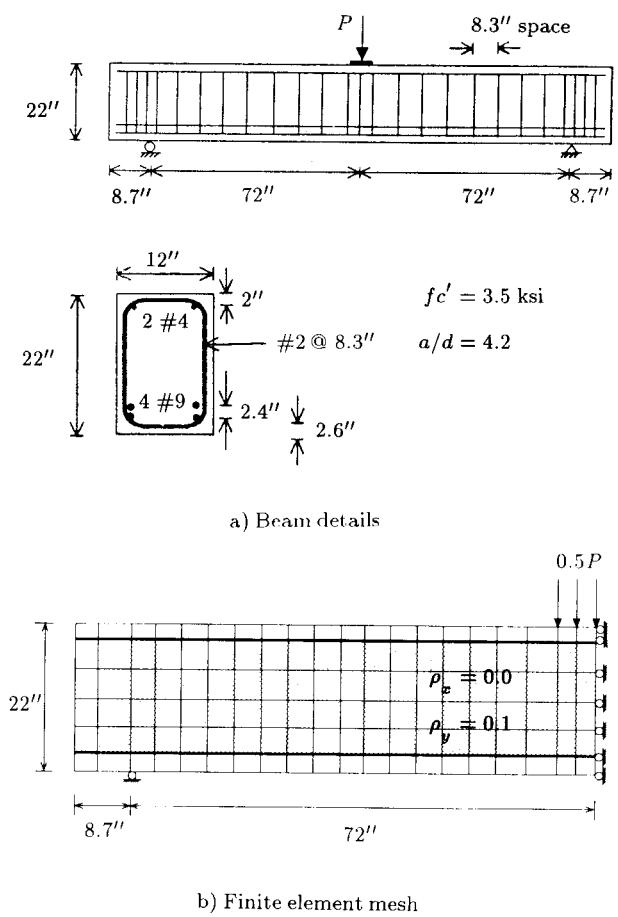

Figure 10. Beam details and finite element model of Bresler and Scordelis beam [20] BS1 (1 in = 25.4 mm, 1 ksi = 6.895 MPa).

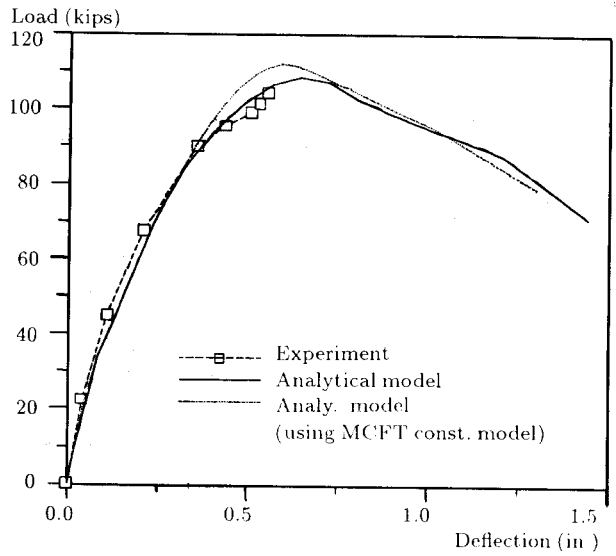

Figure 11. Comparison of analytically predicted and experimentally observed load deflection response of beam with web reinforcement (1 in = 25.4 mm, 1 kip = 4.448 kN).

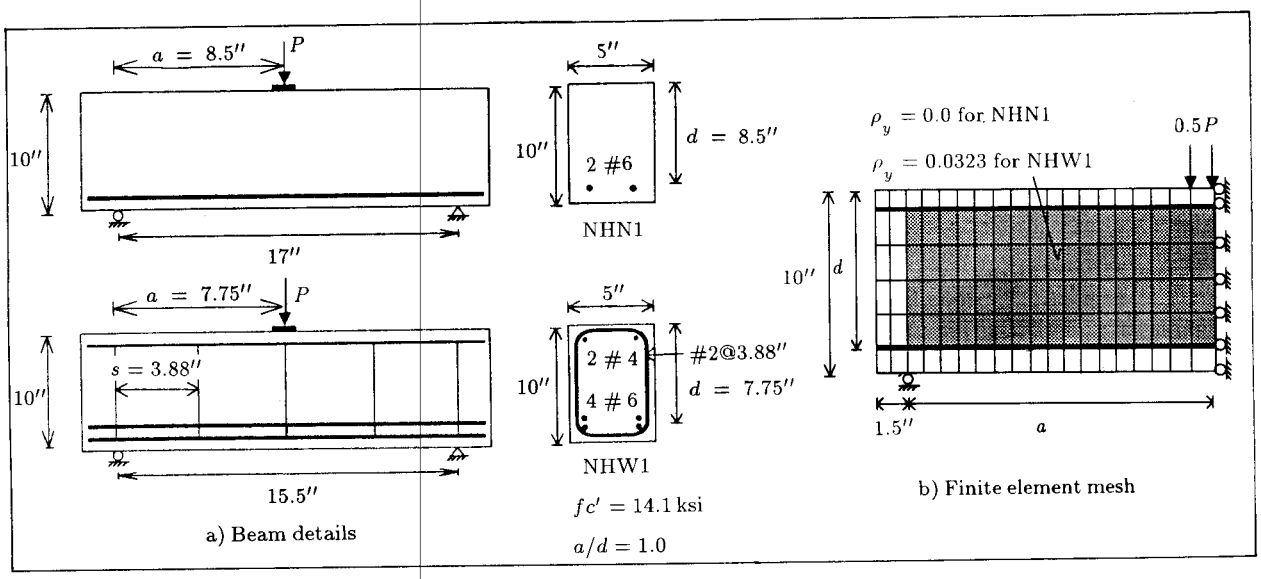

Figure 12. Beam details and finite element model of NCSU beams (1 in = 25.4 mm, 1 ksi = 6.895 MPa).

using the MCFT constitutive model are in good agreement with experimental results, since the web reinforcement ratio is relatively large ($\rho_y = 0.1$) and the section is heavily reinforced.

A number of shear critical reinforced concrete beams utilizing high strength concrete were tested at North Carolina State University [21] to obtain the post-peak load-displacement response. These beams were tested by using an energy absorbing "stiff" testing facility developed at North Carolina State University to test shear critical beams. The details of the test facility are presented in a research report [21]. The beam details of two test beams are described in Figure 12.

The beams were simply supported and subjected to a concentrated load at the mid span. For both of the beams, the compressive strength of the concrete (σ_0) from 150×300 mm. (6×12 in) companion cylinder tests was 14.1 ksi (97.2 MPa). The shear span to depth ratio (a/d) of two beams was 1.0. The beam NHN1 had no stirrups in the shear span and was singly reinforced, while the beam NHW1 had stirrups (no. 2 smooth bar) in the shear span ($\rho_v = 3.79 \times 10^{-3}$) and the longitudinal steel reinforcement consisted of no. 6 bars as tension reinforcement and no. 2 bars as compression reinforcement.

Due to symmetry, half the beam was modelled using 114 rectangular elements. The longitudinal reinforcement was modelled in a discrete manner using the bar elements, while the shear reinforcement was modelled as a smeared element. The tensile strength (f'_t) used in the model was taken as $4\sqrt{\sigma_0}$.

The predicted results using the constitutive model developed in this study are in good agreement with the experimental data, Figures 13 and 14. The predictions of the MCFT constitutive model are not in agreement with the experimental results, since the MCFT constitutive model was developed with experimental data utilizing normal strength concretes and sections which were heavily reinforced. The relatively stiffer predictions in the initial portion of the load-displacement response indicate that the MCFT constitutive model applicability to high strength concrete is questionable. These results furthur indicate that the MCFT is applicable only for heavily reinforced members and it appears that it is not applicable to lightly reinforced or unreinforced concrete members. It should also be recognized that there is a very limited amount of experimental data regarding the complete load-deflection response of shear critical beams of the normal as well as high strength concrete and, as more data becomes

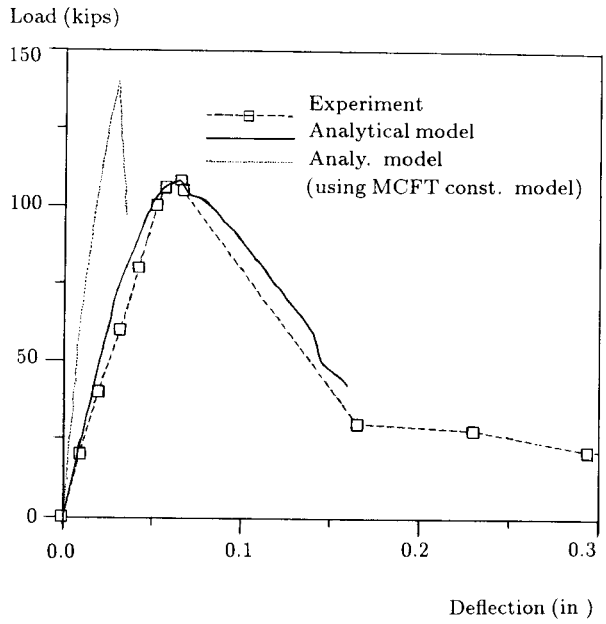

Figure 13. Comparison of analytically predicted and experimentally observed load deflection response of beam without web reinforcement (1 in = 25.4 mm, 1 kip = 4.448 kN).

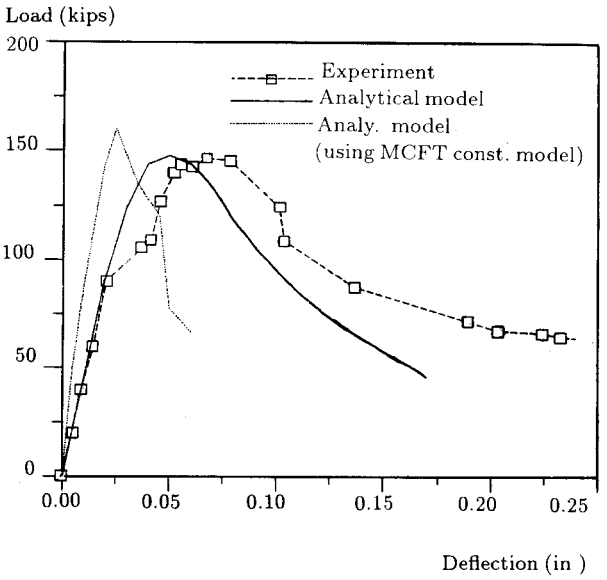

Figure 14. Comparison of analytically predicted and experimentally observed load deflection response of beam with web reinforcement (1 in = 25.4 mm, 1 kip = 4.448 kN).

available, the validity of the model developed in this study can be more throughly evaluated.

SUMMARY AND CONCLUSION

In this investigation, a nonlinear finite element model was developed for predicting the complete load-deflection response of reinforced concrete members. The finite element model is applicable to a short term loading and utilizes plan stress elements with smeared stiffness approach for modeling of the reinforcement. The constitutive model for concrete employs a biaxial stress-strain law which is also applicable to higher strength concretes.

The main feature of the finite element model is its ability to predict the post-peak load deflection response of reinforced concrete members failing under diagonal tension. The model employs the secant displacement increment method and the non-iterative algorithm, which is very efficient in computational time. The predictions of the finite element model are compared with the available experimental data and the comparisons are judged to be in good agreement.

NOMENCLATURE

A, B	ascending and descending parameters
A_c	area of concrete
A_s	steel area
a/d	shear span-depth ratio
d_b	diameter of bar
E_c	concrete modulus
E_s	secant modulus of steel
f_c	compressive stress in concrete
f_s	steel stress
f_t	concrete tensile stress
f'_t	maximum tensile stress
f_y	steel yield stress
G_c	shear modulus
MCFT	Modified Compression Field Theory
SF	step factor

w	concrete weight
α	ρ_s/d_b (in mm)
δ_i	a current displacement step at the assigned node
ε_0	strain at maximum uniaxial stress
ε_{1p}	strain at maximum stress under biaxial stresses
ε_s	strain in steel
ε_{sy}	steel yield strain
ε_t	concrete tensile strain
ε_t	maximum tensile strain in concrete
λ_t	rate of decay parameter
μ	shear retention factor, $0 < \mu \leq 1$
ρ_s	A_s/A_c = longitudinal tensile steel ratio
ρ_v	shear reinforcement ratio
σ_0	uniaxial compressive strength
σ_{1p} & σ_{2p}	peak strength in axis 1 and 2

REFERENCES

1. Vecchio, F.J. and Collins, M.P. "The modified compression-field theory for reinforced concrete elements subjected to shear", *ACI Structural J.* **83**(3), pp 219–231 (1986).

2. Hsu, T.T.C. "Softened truss model theory for shear and torsion", *ACI Structural J.*, **85**(6), pp 624–634 (1988).

3. Kotsovos, M.D. "Behavior of reinforced concrete beams with a shear span to depth ratio between 1.0 and 2.5", *J. of the ACI, Proceedings*, **81**(3), pp 279–286 (1984).

4. Kotsovos, M.D. "Compressive force path concept basis for reinforced concrete ultimate limit state design", *ACI Structural J.*, **85**(1), pp 68–75 (1988).

5. COPPE and CEB. *Colloquium on the CEB-FIP MC90, Department of Civil Engineering*, COPPE/UFRJ Centro de Tecnologia, Brazil, pp 171–188 (1991).

6. Ahmad, S.H. and Shah, S.P. "Complete stress-strain curve of concrete and nonlinear design", *Nonlinear Design of Concrete Structures*, CSCE-ASCE-ACI-CEB International Symposium, University of Waterloo, Ontario, Canada, pp 61–81 (1979).

7. Ahmad, S.H., Shah, S.P. and Khaloo, A.R, "Orthotropic model of concrete for triaxial stresses", *J. of Structural Eng.*, **112**(1), pp 165–181 (1986).

8. Tasuji, M.E., Slate, F.O. and Nilson, A.H. "Stress-strain response and fracture of concrete in biaxial loading", *J. of the ACI*, **75**(7), pp 306–312 (1978).

9. Liu, T.C.Y., Nilson, A.H. and Slate, F.O. "Biaxial stress-strain relations for concrete", *J. of the Structural Division, ASCE*, **98**(5), Proc. Paper 8905, pp 1025–1034 (1972).

10. Kupfer, H.B. et al. "Behavior of concrete under biaxial stresses", *J. of the ACI*, **66**(8), pp 656–666 (1969).

11. Gopalaratnam, V.S. and Shah, S.P. "Softening response of plain concrete in direct tension", *J. of the ACI*, **82**(3), pp 310–323 (1985).

12. Stevens, N.J., Uzumeri, S.M., Collins, M.P. and Will, G.T. "Constitutive model for reinforced concrete finite element analysis", *ACI Structural J.*, **88**(1), pp 49–59 (1991).

13. Dodds, R.H., Darwin, D.M. and Leibengood, L.D. "Stress controlled smeared cracking in R/C beams", *J. of Structural Eng.*, ASCE, **110**(9), pp 1959–1976 (1984).

14. Pramono, E. "Numerical simulation of distributed and localized failure in concrete", Thesis presented to the faculty of the graduate school of the University of Colorado in partial fulfillment of the requirements for the degree of Doctor of Philosophy, Dept. of Civil, Environmental, and Architectural Engineering (1988).

15. Vecchio, F.J. "Reinforced concrete membrane element formulations", *J. of Structural Eng.*, ASCE, **116**(3), pp 730–750 (1990).

16. ASCE, *Finite Element Analysis of Reinforced Concrete*, New York, pp 545 (1982).

17. Weaver, Jr., W. and Johnston, P.R. *Finite Elements for Structural Analysis*, Prentice-Hall, Inc., Englewood Cliffs, N.J. USA (1984).

18. Chung, W. "Analytical model for diagonal tension failure of reinforced concrete members under static loads", Ph.D. thesis, North Carolina State University (1992).

19. Leonhardt, F. and Walther, R. "Wandartige Träger", Bulletin No.178, Deutscher Ausschuss fur Stahlbeton, Berlin, pp 159 (1966).

20. Bresler, B. and Scordelis, A.C. "Shear strength of reinforced concrete beams", *J. of the ACI, Proceedings*, **60**(1), pp 51–74 (1963).

21. Xie, Y., Hino, S. and Chung, W. "Testing facility for controlled diagonal tension of shear critical reinforced concrete beams", Research Report, Department of Civil Engineering, North Carolina State University, Raleigh, NC 27695 (Oct.–Nov. 1992).